International Conference on Space Optics—ICSO 2022

Dubrovnik, Croatia

3–7 October 2022

Edited by Kyriaki Minoglou, Nikos Karafolas, and Bruno Cugny,

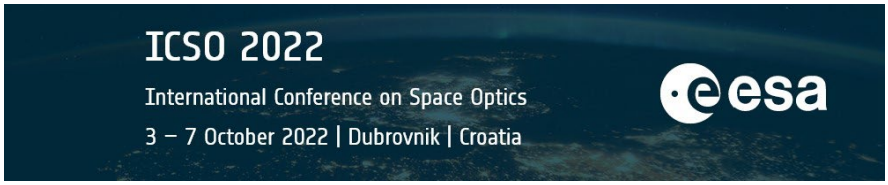

Short Comb Atmospheric Lidar Experiment (SCALE): principles, activities at CNES and perspectives for a new LIDAR concept

International Conference on Space Optics — ICSO 2022, edited by Kyriaki Minoglou, Nikos Karafolas, Bruno Cugny, Proc. of SPIE Vol. 12777, 127772U · © 2023 ESA and CNES · 0277-786X · doi: 10.1117/12.2690305

Short Comb Atmospheric Lidar Experiment (SCALE): principles, activities at CNES and perspectives for a new LIDAR concept

M. Costella*[a], J. Roubichou[a], M. Boutillier[a], N. Maron[a,b], R. Arguel[a], P. Lafrique[a] P, A. Materne[a], P.J Hébert[a], V. Pascal[a], V. Tyrou[a]

[a]CNES, Centre National d'Etudes Spatiales, 18 Av. Edouard Belin, 31400, Toulouse
[b]SYRTE, Observatoire de Paris, Université PSL, CNRS, Sorbonne Université, LNE, Paris, France.

ABSTRACT

This paper presents a new concept of frequency comb LIDAR instrument for atmospheric CO2 mapping. The French space agency (CNES) has initiated the development of an airborne proof of concept. The main originality of this instrument lies in the use of two probe combs crossing the same atmospheric path and used for self-phase correction. This technique, named Double Heterodyne Detection (DHD), allows us to coherently average interferograms beyond the coherence time of the laser source. The LIDAR airborne instrument is designed for real-conditions atmospheric CO_2 measurements at 1.572 µm and mainly relies on commercial telecom components. We present experimental results on a breadboard laboratory version of the instrument and our data processing method. Then, we extend the study to a space instrument and provide a first estimation of radiometric performances.

Keywords: Heterodyne LIDAR, frequency comb, Dual-comb spectroscopy

1 INTRODUCTION

1.1 SCALE concept at CNES

Dual Comb Spectroscopy principle with short frequency combs (only a few teeth are generated by the phase modulation of a continuous wave laser) opens the path to a new generation of LIDAR instruments, potentially usable in airborne or space greenhouse gases sounding missions. Short frequency combs scan a whole absorption line of the target molecule with a near-perfect mastering of the spectral pattern. Thus, the main advantage of short combs is to relax the highly accurate frequency calibration needed in the case of DIAL LIDARS, especially for CO_2 sounding. More generally, it allows for a retrieval processing based on Bayesian optimal estimation that can deal with several technical or geophysical unknowns, thanks to the spectral richness and accuracy of the signal. After a series of R&D studies carried out by ONERA and CNES on frequency comb LIDARS[1,2], CNES has initiated the development of an Exploratory Project (also known as « PEX ») in CNES. Exploratory Projects are a new innovative category of projects set up in CNES a few years ago, which are limited in time and budget and specially designed to test innovative technologies. They are based on a pragmatic approach focused on the demonstration objective, and are designed and developed internally in CNES. SCALE Exploratory Project has been decided in July 2020 and started in September 2020, for an airborne demonstration planned in July 2023. It aims at demonstrating the feasibility and the performance of two innovations patented by CNES: the use of short frequency combs for atmospheric sounding, and the improvement of SNR obtained through Double Heterodyne Detection.

These two innovations have been studied and validated in lab environments through research activities performed between 2014 and 2019 with ONERA. The combination of these two innovations is believed to bring a breakthrough in atmospheric sounding, thanks to the improved richness of the information retrieved with short combs (compared to IPDA LIDARs), the relaxation of frequency knowledge constraints and the improvement of SNR. A system level Phase 0 Study has been conducted in CNES in 2019 and concluded that the performance budget shows a good balance between the contributors and would be compliant with the objective of 1ppm CO2 retrieval over 50km. However, theory and literature could not give answers to all the performance questions raised (impact of the Speckle effect, DHD mixing performance, turbulence

for vertical shots…). Thus, confrontation with an airborne system experiment was necessary to test performances in a mode representative configuration before moving on to a Space Project. In parallel, a simplified Lab-POC (Proof Of Concept) has been developed in the Optics Lab from the beginning of the PEX. It is used to perform the validation of different set points for the Airborne-POC, the study of specific technical aspects such as speckle and to enable SCALE teams to generate the representative signals required to develop and optimize the signal processing algorithms, which are key to reaching the targeted performance.

1.2 SCALE airborne demonstrator

The Airborne POC of SCALE will fly in July 2023 on a Commercial ATR42 Aircraft from the SAFIRE fleet. This ATR42 has been specially modified for atmospheric measurements and is used regularly for scientific experiments. The SAFIRE fleet is located in Francazal near Toulouse, and is funded by CNES, Meteofrance and CNRS. SCALE Airborne Proof of Concept is currently under development in CNES, supervised by the project team and CNES experts from different sub-directorates. All subsystems are now contracted, and the first deliveries have been received and verified in the CNES Optics Laboratory, progressively building up the Airborne-POC. A series of scientific equipment will be present on board the aircraft, and scientific means set up on-ground and in balloons on the trajectory of the ATR42, to derive the reference CO2 mixing ratios to be compared with SCALE processed data.

In parallel to the PEX, a Phase 0 with Airbus Defense and Space has started early 2022 and is planned to end in 2023. Its aim is to study the feasibility and any instrument design improvement required to target a space mission with a SCALE instrument on-board for Greenhouse gases measurements. The results of this Phase0 study, combined with the results and lessons learned of the PEX, will open the way to a Spaceborne SCALE study.

2 DUAL COMB SPECTROSCOPY APPLIED TO A LIDAR

The SCALE optical architecture mainly relies on a dual comb spectrometer[3–5]. The architecture of the breadboard instrument is depicted in Figure 1 : optical architecture of the SCALE instrument. Frequency combs of the local oscillator and two probe beams are obtained with electro-optic modulation (EOM) [6] of a single fibered laser (Master Oscillator). To obtain a good compromise between the spectral richness of the comb and the optical power in each tooth of the comb, we chose to create seven teeth optical combs. Then, each comb is frequency shifted with acousto-optic modulators. Furthermore, amplitude modulation of the RF (radio-frequency) signal applied to each AOM on the probe path allows us to send a pulsed signal through the atmosphere, to measure accurately the flight time between the signal sent and the echo. On the airborne demonstrator, an optical fiber amplifier will amplify the two probe beams, providing an average optical output power of 1W. Then, a monostatic telescope focuses the two probe combs on a target, and the echo signal is mixed with the local oscillator on a high-speed detector. The RF signal induced by the heterodyne mixing of the Local Oscillator (LO) comb with the two probes is filtered, digitized, and recorded for post-processing.

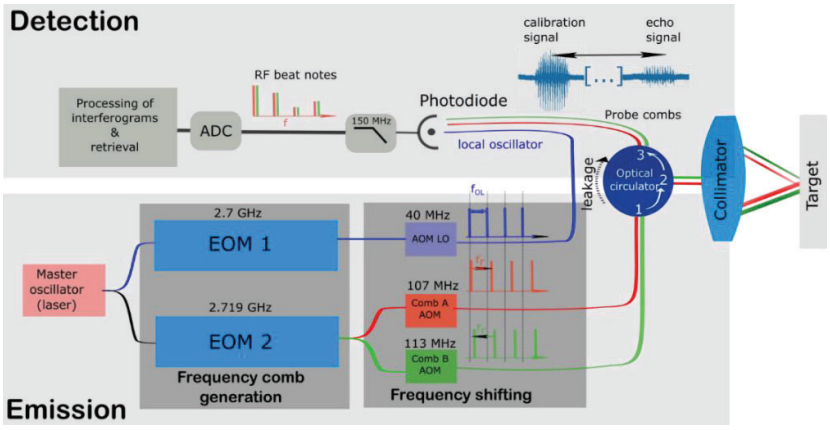

Figure 1 : optical architecture of the SCALE instrument

The spectrum of the signal registered on the photodetector is composed of two frequency combs in the 10-150 MHz range. In order to deal with non-flat combs such as EOM combs, a calibration signal is registered at each optical pulse emission. Then, the absorption spectrum is obtained by dividing the measurement spectrum by the calibration spectrum. This paper will present different signal processing methods, including the DHD, which uses a second digital heterodyne beat note by mixing the RF signal of each probe combs. The two probe combs undergo the same random phase induced by the laser source and atmospheric turbulences. With DHD, this random phase can be removed by post-processing so that the integration time is no longer limited by the laser coherence time and atmospheric turbulences, offering a great advantage over classical heterodyne detection. This paper will also discuss how to overcome the Speckle issue in the particular case of frequency combs when the probe beams reflect on a rough surface. To finish, technical perspectives and foreseen performances of a future space application will be discussed.

2.1 Heterodyne signal on the detector

Considering a k^{th} teeth in the first probe comb (comb A) and the LO comb, the current induced on the photodetector is

$$\mathrm{i_{HAk}} = \mathrm{S}.(P_{LOk} + P_{Ak}) + 2.\mathrm{S}.\sqrt{\gamma_\mathrm{H}.\mathrm{P_{LOk}}.\mathrm{P_{Ak}}}.\cos(2\pi(\nu_\mathrm{Ak} - \nu_\mathrm{LOk}).\mathrm{t}) \quad \text{Equation 1}$$

Where P_{LOk} is the power of the k^{th} tooth of the LO comb [W], P_{Ak} is the power of the k^{th} tooth of the 1^{rst} probe comb [W], S is the sensitivity of the detector [A/W], γ_H is the heterodyne mixing efficiency, ν_Ak is the frequency of the k^{th} tooth of the 1^{rst} probe comb [Hz], ν_LOk is the frequency of the k^{th} tooth of the local oscillator comb [Hz], and t is the time [s]. The DC part of this signal is filtered before digitizing. The total signal digitized, for order k, after proper filtering, is composed of the superposition of heterodyne beat notes of LO and comb A (noted $\widetilde{\imath_{\mathrm{HAk}}}$) and the beat note of LO and comb B (noted $\widetilde{\imath_{\mathrm{HBk}}}$):

$$\widetilde{\imath_{\mathrm{Hk}}} = \widetilde{\imath_{\mathrm{HAk}}} + \widetilde{\imath_{\mathrm{HBk}}} \quad \text{Equation 2}$$

Where $\widetilde{\imath_{\mathrm{HAk}}}$ and $\widetilde{\imath_{\mathrm{HBk}}}$ are the AC current:

$$\begin{cases} \widetilde{\imath_{\mathrm{HAk}}} = 2.\mathrm{S}.\sqrt{\gamma_\mathrm{H}.\mathrm{P_{LOk}}.\mathrm{P_{1k}}}.\cos(2\pi(\nu_\mathrm{1k} - \nu_\mathrm{LOk}).\mathrm{t}) \\ \widetilde{\imath_{\mathrm{HBk}}} = 2.\mathrm{S}.\sqrt{\gamma_\mathrm{H}.\mathrm{P_{LOk}}.\mathrm{P_{2k}}}.\cos(2\pi(\nu_\mathrm{2k} - \nu_\mathrm{LOk}).\mathrm{t}) \end{cases} \quad \text{Equation 3}$$

As a result, the power spectral density of the total digitized signal is a comb composed of seven pair of peaks (k = -3,…3) , each peak inside a pair corresponding to the probe comb A and B, respectively. As comb A and comb B have very close optical frequencies, (6 MHz difference), we can consider that each peak inside a pair is equally absorbed by the atmosphere.

2.2 Data processing for phase noise correction

Laser phase noise and phase noise induced by atmospheric turbulences limits the integration time of the signal. However, to obtain a good SNR, it is necessary to average a large number of temporal signals (with a random phase). To remove this frequency noise and coherently average a large number of interferograms, one solution is to choose a reference peak and extract the temporal evolution of its phase for the phase correction. As the probe combs come from the same laser source and cross the same atmospheric turbulences, their frequency noise is almost similar all along the spectrum, and the random phase cancels by correcting the whole signal by the phase of the reference peak[7]. However, in real condition, the Speckle could affect differently each order of the comb, making it impossible to phase-correct all the comb by only one of its line. To address this issue, we use two probe combs, and make a second heterodyne mixing between the two same order peaks of probe comb A and probe comb B. After numerical filtering of each pair of peaks, the principle of this data processing method called DHD is to calculate, at each time sample t, the square of $\widetilde{\imath_{\mathrm{Hk}}}$:

$$\widetilde{\imath_{\mathrm{Hk}}}^2 = (\widetilde{\imath_{\mathrm{H1k}}} + \widetilde{\imath_{\mathrm{H2k}}})^2 = \widetilde{\iota_{HAk}}^2 + \widetilde{\iota_{HBk}}^2 + 2.\widetilde{\iota_{HAk}}.\widetilde{\iota_{HBk}} \quad \text{Equation 4}$$

For each comb, the frequency of a k-order tooth is affected by a frequency noise Δυ and a random phase φ. Numerical filtering keeps the lowest frequency of the last term of Equation 4 only. By replacing $\iota_{\widetilde{HAk}}$ and $\iota_{\widetilde{HBk}}$ by their expression given in Equation 3, the low frequency part of this last term can be written as:

$$\widetilde{\iota_{\mathrm{Hk}}}^{2}{}_{LF} = 4.S^2.\gamma_H.P_{LOk}.\sqrt{P_{Ak}.P_{Bk}}.cos(2\pi.((\nu_{Ak}+\Delta\nu_{Ak}+\varphi_{Ak})-(\nu_{Bk}+\Delta\nu_{Bk}+\varphi_{Bk})t) \quad \text{Equation 5}$$

Each peak of a pair comes from the same optical source, travel almost the same optical path, and have very close optical frequencies (6 MHz difference). Thus, $\Delta\nu_{Ak} = \Delta\nu_{Bk}$ and $\varphi_{Ak} = \varphi_{Bk}$. The common phase and frequency noise on each probe comb cancels, and Equation 5 becomes:

$$\widetilde{\iota_{\mathrm{Hk}}}^{2}{}_{LF} = 4.S^2.\gamma_H.P_{LOk}.\sqrt{P_{Ak}.P_{Bk}}.cos(2\pi.(\nu_{Ak}-\nu_{Bk})t) \quad \text{Equation 6}$$

The difference between optical frequencies ν_{Ak} and ν_{Bk} is determined by the frequency difference on the RF signals applied on AOM A and AOM B. In practice, this difference is few MHz, reducing the signal bandwidth ΔB from hundreds of MHz for the complete heterodyne spectrum (and several GHz for the optical spectrum) to only few MHz for the final useful electrical signal.

3 EXPERIMENTAL SETUP AND PRELIMINARY RESULTS ON THE LAB POC

The optical architecture of the lab POC is in Figure 1. The laser source used is a fiber laser FITEL FRL15DCWD centered around 1545 nm. The choice of the laser source is made according to the atmospheric absorption line sounded. A current controller (ILX Lightwawe, LDX-3412) and a temperature controller (ILX Lightwave, LDT-5412) control the laser central wavelength. The optical linewidth of this fibered diode is 1MHz. Then, a 50/50 fibered coupler splits the light into two parts, two combs with slightly different repetition rates are created (2.7 and 2.718 MHz with electro-optic modulation (iXblue, MPZ-LN-01). The LO comb is 40 MHz frequency shifted with an acousto-optic modulation (AOM) (Gooch & Housego). The second comb is split into two probe combs, each comb is shifted by 107 and 113 MHz. To simulate an absorption line, the two probe beams are combined in a fibered Bragg band-cut filter. Then, we studied two configurations. In the first configuration (all-fibered), the two probe beams are recombined with the LO comb on a high-speed PIN photodiode (Gooch & Housego, DS-7064). In the second configuration, with an open space part in the layout, we studied the effect of the reflection of the probe beams on a surface with random roughness. The two probe-combs fiber is connected on Port 1 of an optical circulator. Port 2 is connected to a collimator, which focuses the probe beams on a frosted metal surface mounted on a small electric motor to renew the reflector surface between each measurement. Then, the reflected light is collected by the same collimator and mixed on the photodetector via Port 3 of the optical circulator. After PD, the signal is filtered by a DC block (MCL, BLK-89-S+) and an anti-aliasing low-pass filter (Minicircuit, VLF-220+).

The radio-frequency signal is digitized with a 1.25 GS/sec 8 bits digitizer (Spectrum Instrumentation, M4i.2211 x8). The probe combs are pulsed with a super-Gaussian shaped temporal envelope with a 3 µs FWHM (Full Width at Half Maximum). The voltage sampled of a pulse is in Figure 2(a), and detailed in Figure 2(b).These pulses are generated by modulating the RF signal applied to AOMs. In the SCALE concept, two acquisitions are made for each measurement. The spectrum of this signal is displayed in Figure 2(c). All useful frequencies are in the 5-140 MHz range. The spectrum is composed of two frequency combs obtained by the heterodyne mixing of LO and comb A, and LO and comb B, respectively. These two combs have a 6 MHz (= 113-107 MHz) frequency spacing and form 7 pair of peaks, from order k = -3 to order k = 3. The first acquisition, regarded as the reference pulse used for calibration, is the signal induced by the optical leak between Port 1 and Port 3 of the optical circulator. The second is an acquisition of a measurement pulse that traveled through the atmosphere.

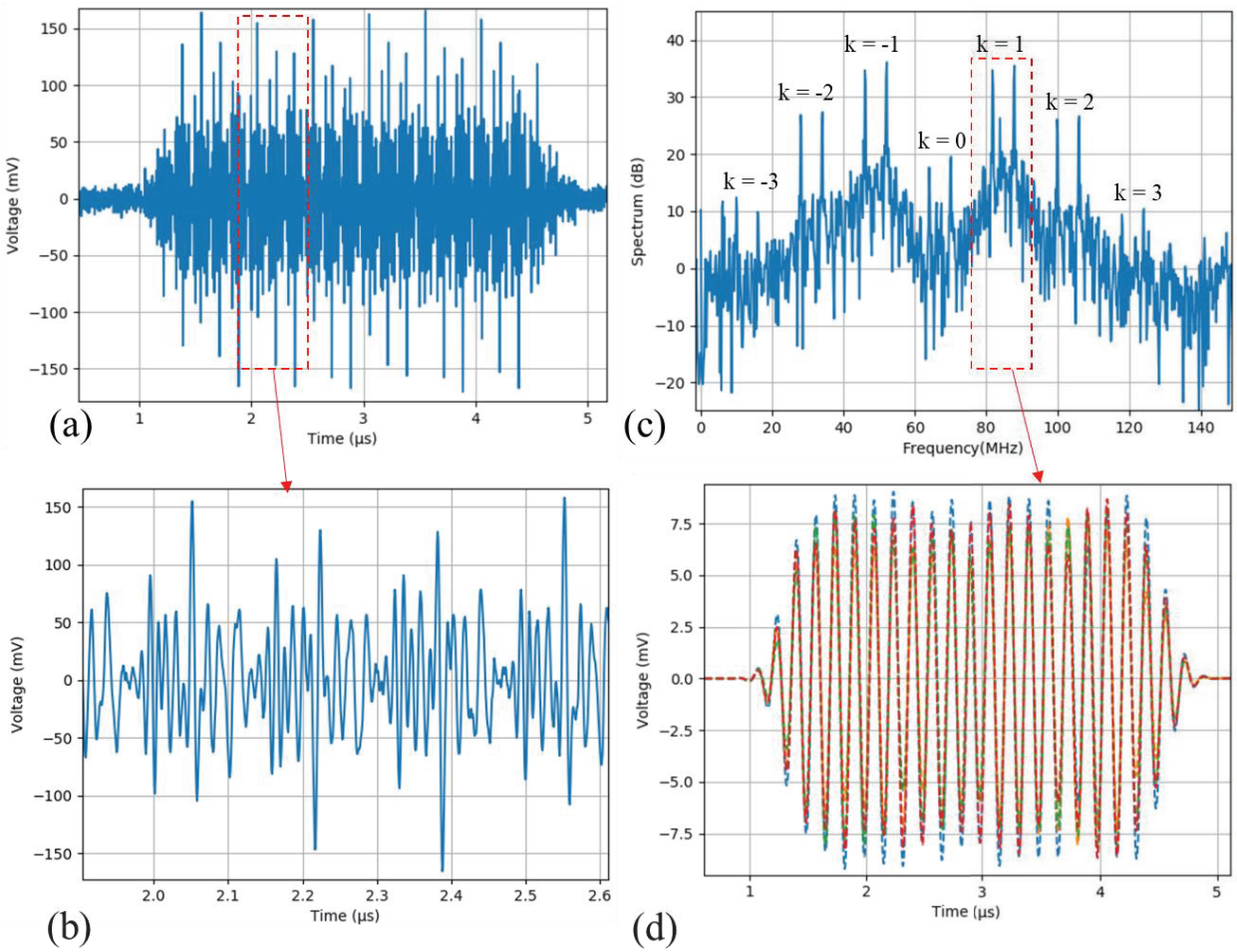

Figure 2 (a): digitized interferogram for one pulse and zoom on patterns (b). (c): Spectrum of the interferogram. (d): low-frequency signal of the k=1 pair of peak, displayed for 4 different measurements.

Figure 3 presents the transmission of the Bragg filter (dashed line) and the same transmission experimentally measured by the SCALE breadboard with two different methods. The averaged values and their standard deviation (dots and error bars) are estimated on 20 measurements, and 250 pulses are averaged for each measurement. Figure 3(a) displays the results for the all-fibered configuration, and Figure 3(b) shows the effect of the Speckle when the probe beams are backscattered by a moving rough surface. For each case, the data set is the same, but we applied two different data processing methods. In the SHD (Single heterodyne detection) method (orange), we simply estimate the energy contained in each spectrum channel of the combs. The green data points show the transmission computed by the DHD method described in the previous section. The use of DHD leads to a significant reduction of the standard deviation of the measure in both measurement configurations, with and without the Speckle effect. For instance, Figure 2(d) shows the low frequency signal described in Equation 6 and obtained by squaring the first order (k = 1) composite signal. This final signal is displayed for 3 successive pulses. As a result, even if the temporal pattern has a phase noise due to decoherence, roughness of the reflection surface, or atmospheric turbulences, the final low-frequency signal exhibits near-perfect phase stability. Thus, this one can be averaged coherently on a large number of pulses, even in the presence of the Speckle effect. To obtain the transmission spectrum in Figure 3, for an order k, the energy contained in the averaged low frequency signal is computed for the measurement and the calibration signal. Then, the measurement value is divided by the calibration value to compensate the non-flat spectral shape of the optical frequency comb.

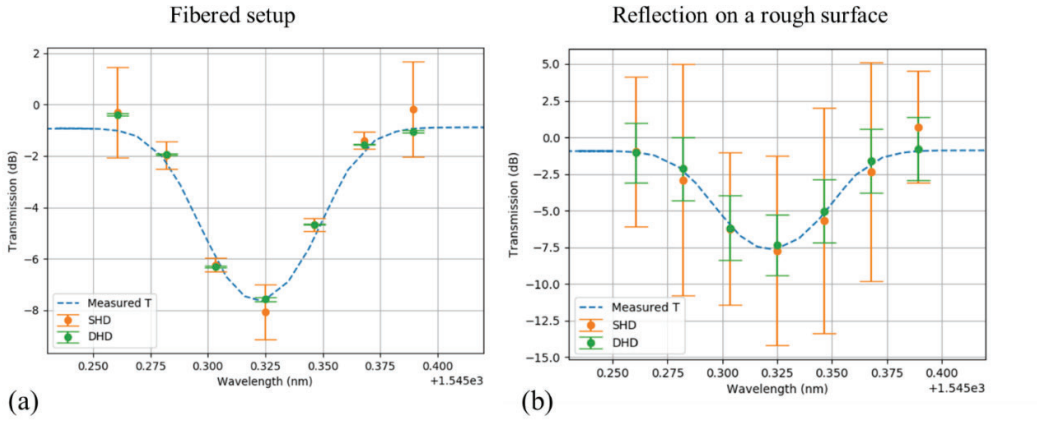

Figure 3 : (a) Measured transmission of the Bragg filter (dashed line) with the classical dual comb spectroscopy (orange) and the Double Heterodyne detection (green). (b): same measurement with a reflection on a rough surface inducing Speckle.

3.1 Time of flight measurement

For an accurate CO2 retrieval, the instrument must be able to measure precisely the optical path traveled by the probe combs. Measuring the time flight between the calibration pulse and the echo pulse gives this parameter. The accuracy on this dating is driven by the precision needed on the concentration of the gas studied. For carbon dioxide, the required accuracy is 1 ppm, or 0.25% in relative. It is thus estimated that an accuracy of 10 ns must be reached for the temporal location of a pulse, or 2.3 µs after averaging of 50,000 shots. The probe combs are pulsed with super-Gaussian shaped temporal envelope. These pulses are generated by modulating acousto-optical modulators (AOM) with a RF signal. In the SCALE concept, two acquisitions are made for each measurement. The first acquisition is the sampling of a leak on board the instrument and considered as the reference pulse. The second is an acquisition of a measurement pulse that travelled through the atmosphere. That pulse was affected byits reflection on the ground by the speckle. Normally used to obtain calibrate measurements, these two signals can be reused to determine the time of flight of photons.

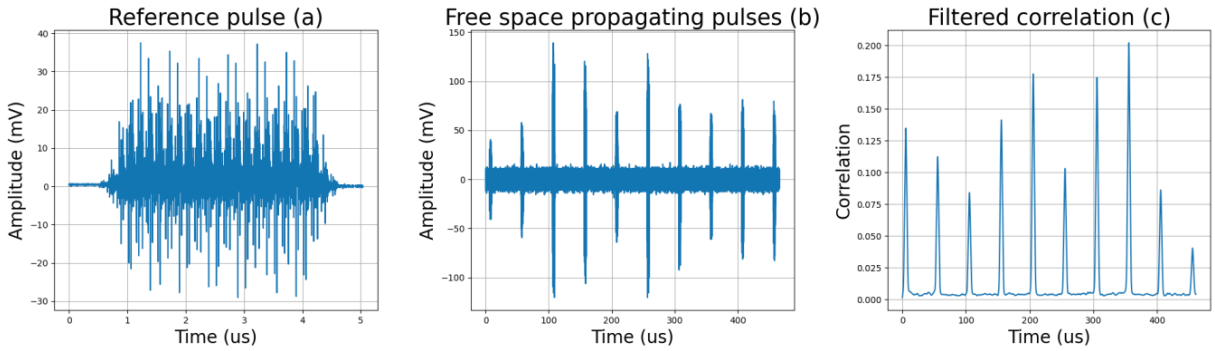

Figure 4: (a) Reference pulse measured on board the instrument without free-space propagation. (b) Series of pulses after their propagation in free-space and degradation by speckle. (c) Filtered correlation between the reference pulse and the series of measurement pulses.

A temporal dating based only on their super-Gaussian envelope would not allow to reach the need since the generated pulses have a 2 µs width at half height. To obtain the desired accuracy, a correlation method based on interferograms contained in reference and measurement pulses has been developed. This technique allows to determine the time of flight with the sufficient accuracy by detecting the maximum correlation between the two measurements. To verify this method, a reference pulse was measured on board the instrument, without free-space propagation as presented in Figure 4(a). At the same time, a series of pulses with controlled time spacing, propagating in free space and distorted by the speckle have

been detected as shown in Figure 4(b). It was thus possible to compare the theoretical time spacing of the pulses with the results of the method, as illustrated Figure 4(c). These preliminary measurements showed that the correlation method led to errors at least four times lower than the theoretical need despite the presence of speckle

4 RADIOMETRIC PERFORMANCE

4.1 Useful Signal to Noise Ratio

We assume that the optical power coming back from the target is the same for the two probe combs, and we call it P_{Sk}:

$$P_{Sk} = P_{Ak} \approx P_{Bk} \quad \text{Equation 7}$$

Equation 6 becomes:

$$\widetilde{\imath_{Hk}}^{2}{}_{LF} = 4.S^2.\gamma_H.P_{LOk}.P_{Sk}.cos(2\pi.(\nu_{Ak} - \nu_{Bk})t) \quad \text{Equation 8}$$

The useful Signal to Noise Ratio (SNR) is about P_{Sk}, i.e. the k^{th} component in the spectrum of the optical power coming from the target:

$$\mathrm{SNR} = \frac{\mathrm{P_{Sk}}}{\sqrt{\mathrm{var(P_{Sk})}}} \quad \text{Equation 9}$$

where $\mathrm{var(P_{Sk})}$ is the variance of the measurement of P_{Sk}. As Equation 8 shows, P_{Sk} is proportional to $\widetilde{\imath_{Hk}}^{2}{}_{LF}$. Thus, $SNR = \frac{\widetilde{\imath_{Hk}(t)}_{LF}}{2.\sqrt{\mathrm{var}(\widetilde{\imath_{Hk}(t)}_{LF})}}$. The useful SNR will be half that of the k^{th} low frequency component of the heterodyne current signal as generated by the detector. Assuming that the noise is white and dominated by shot noise, and considering combs of $N_{teeth} = 7$ teeth, with an evenly distributed power on them, we can express the SNR as a function of the total heterodyne current at time t = 0, including all its spectral components:

$$SNR = \frac{\widetilde{\imath_H(0)}_{LF}}{2.\sqrt{N_{teeth}.\mathrm{var}(\widetilde{\imath_H(0)}_{LF})}} = \frac{1}{2.\sqrt{N_{teeth}}}.SNR_{\widetilde{\imath_H}} \quad \text{Equation 10}$$

4.2 Radiometric SNR on heterodyne current

The received signal power is close to:

$$2.P_S = P_A + P_B \quad \text{Equation 11}$$

as it is the sum of the two probe beams of equal powers. P_S is the power of each received combs, all spectral components included. At time t = 0, all the beat tones are in phase and the current has the value:

$$\widetilde{\imath_H(0)} = 2.S.\sqrt{2.\gamma_H.P_{LO}.P_S} \quad \text{Equation 12}$$

The different shot noise sources generate the signal variances:

- for the useful signal: $2.q.\Delta B.F.S.2.P_S$
- for the background of sun radiance backscattered by the ground: $2.q.\Delta B.F.S.P_{BG}$
- for the local oscillator flux : $2.q.\Delta B.F.S.P_{LO}$

with: q = electron charge [C]
ΔB = the final bandwidth of the signal, after DHD process is applied;
F = excess noise factor of the detector;
P_{BG} = optical power of sun radiance backscattered by the ground;
P_{LO} = optical power of the local oscillator onto the detector.

The detector dark current gives rise to the signal variance: $2.q.\Delta B.F.I_{dark}$ where I_{dark} is the dark current generated by the detector. The main current noise after the detector is due to the first stage amplifier, a Resistor Trans Impedance Amplifier (RTIA). Back propagated to the output of the detector, the variance that the RTIA generates is:

$$2.q.\Delta B.\frac{I_{b\_RTIA}}{G}$$

Where G is the gain of the RTIA; and I_{b_RTIA} is the noise current generated at the output of the RTIA. Finally, the radiometric part of the SNR in the heterodyne current is thus:

$$SNR_{\overline{i_H}}^{rad} = 2\sqrt{\frac{S^2.\gamma_H.P_{LO}.P_S}{q.\Delta B.S.F.(P_{LO}+2.P_S+P_{BG})+q.\Delta B.I_{obs}+q.\Delta B.\frac{I_{b\_RTIA}}{G}}} \quad \text{Equation 13}$$

In the case where the local oscillator power is larger than the other signals, this expression becomes:

$$SNR_{\overline{i_H}}^{rad} \approx 2.\sqrt{\frac{S.\gamma_H.P_S}{q.\Delta B.F}} \quad \text{Equation 14}$$

Equation 14 depicts a photon noise limited, direct detection, situation, with the drawback of a $\gamma_H < 1$ heterodyne mixing efficiency. On the other hand, DHD allows a detection bandwidth as low as a few MHz.

4.3 Effect of speckle

Noise due speckle adds quadratically to radiometric noise:

$$SNR = \frac{1}{2}\frac{1}{\sqrt{\left(\frac{1}{SNR^{sp}}\right)^2+\left(\frac{\sqrt{N_{teeth}}}{SNR_{\overline{i_H}}^{rad}}\right)^2}} \quad \text{Equation 15}$$

As shown in [8], the speckle adds noise to the measurement, and the spectral components are uncorrelated provided that they are spaced by a sufficient frequency gap, and/or the roughness of the backscattering is bigger than a few mm. This is the case in SCALE as it uses the reflection on the ground onto a footprint of 2 m diameter. As is the case with coherent detection, the SNR due to Speckle, if one considers a single shot on a rough surface, is:

$$SNR^{sp} = 1$$

When N_{shot} shots, with a renewal rate of τ_{renew} are averaged, the total SNR, averaged in the spectrum, becomes:

$$SNR = \frac{1}{2}.\frac{\sqrt{N_{shot}}}{\sqrt{\left(\frac{1}{\tau_{renew}}\right)^2+\left(\frac{\sqrt{N_{teeth}}}{SNR_{\overline{i_H}}^{rad}}\right)^2}} \quad \text{Equation 16}$$

τ_{renew} is given by: $\tau_{renew} \approx \frac{V_{sat}}{\Phi_{pixel_{ground}}.F_c}$ if $V_{sat} < \Phi_{pixel_{ground}}.F_c$; = 1 otherwise; where V_{sat} is the velocity of the satellite, Φ_{pixel_ground} is the diameter of the laser footprint on ground, and F_c is the pulse repetition frequency, as illustrated in Figure 5:

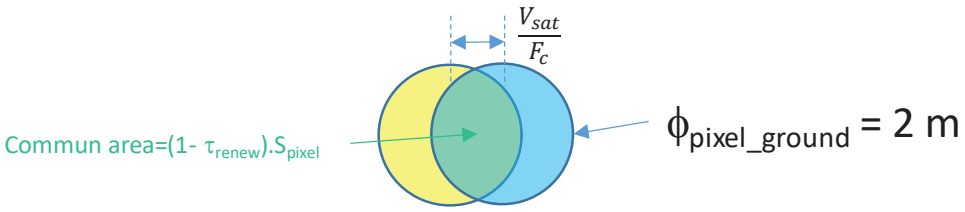

Figure 5: renewal rate of successive spots on ground

Because of Equation 16, the final SNR is limited by the worse of radiometric noise and speckle noise. The latter being equal to 1, there is no use having a radiometric SNR much better than 1 on a single shot. On the contrary if $SNR_{i_H}^{rad} \ll 1$, the total SNR will be limited by this low value.

5 ASSUMPTIONS ON MAIN RADIOMETRIC PARAMETERS FOR A SPACE MISSION

Figure 6 illustrates the main parameters applied in the above equation to establish a preliminary radiometric performance for a space mission:

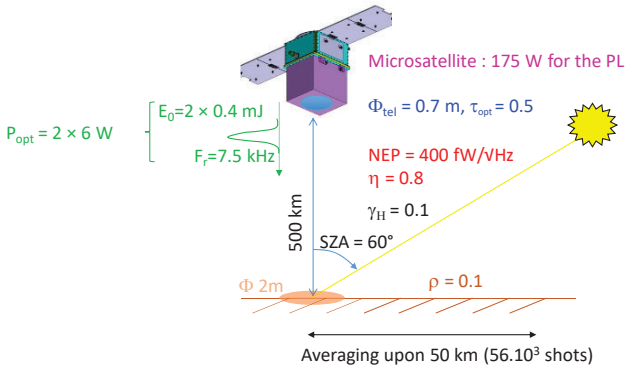

Figure 6: main setting radiometric parameters

The main issue of the radiometric budget is the output optical power of 6W for each probe comb. We assume that we can obtain them, moreover with a wall-plug efficiency of 11 %. Obviously, these figures will need some developments to be met, but [9] shows some results close to them. This power provides pulse energy of 0.4 mJ at 7.5 kHz for each comb. The telescope has a diameter of 0.7 m and the optics have a global transmission of 50 %. The detector is characterized by a NEP (Noise Equivalent Power) of 400 fW/√Hz and η = 0.8 quantum efficiency. We consider a classic photodiode with F = 1, as opposed to an APD with F close to 3. Indeed the impact of F > 1 is bigger than the advantage of the magnification in an APD in the overall budget. The heterodyne mixing efficiency is supposed to be γ_H = 0.1. For the calculation of the return flux, we assume an albedo ρ = 0.1 on the ground and 56,000 shots averaged along 50 km. Given these assumptions the peak power received from the ground is $0.8.10^{-11}$ W < P_S <2.10^{-11} W, depending on the margins taken into account. The local oscillator is CW with a power of 110 µW to 600 µW. For the final signal bandwidth ΔB, we take a value of 4 MHz into account in place of 6 MHz in the airborne POC.

Our first study with the above model gives the SNR values displayed in Figure 7. The high laser pulse repetition frequency allows getting measurements with a better on-ground resolution, but with a degraded SNR, following a square root law. . The key parameter remains the optical power of the emitter. The diameter of the telescope is limited by the platform size and the difficulty to keep a high γ_H with a large telescope. In our budget, Figure 7 (right) shows the weight of each item discussed in the previous sections. By far, the shot noise is predominant. One point of note is that improving the radiometric performance far beyond the assumptions above would have a limited effect, as the measurements would be dominated by the Speckle noise. Other system studies led by CNES show that an SNR of 100 would be optimal for CO_2 retrieval, given

the other sources of error that cannot be reduced, such as the spectroscopy knowledge of CO_2 or surface pressure measurement. For the time being, assumptions taken on the budget parameters need to be worked out to reduce the uncertainties, or to improve the low estimate, in the Figure 7 graph.

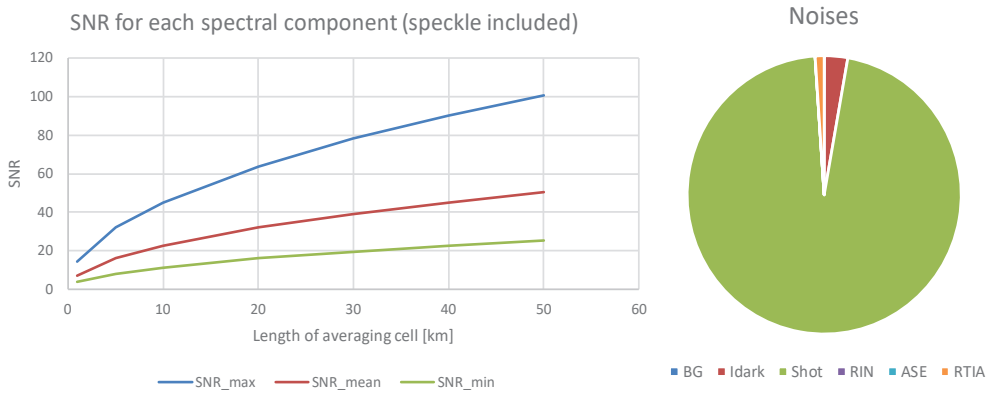

Figure 7 : SNR for each spectral components (left) and relative weight of different sources of noise (right)

6 REFERENCES

[1] Hébert, P. J. and Lemaître, F., "SCALE: validations and prospects for a novel type of sounding lidar using short frequency combs," International Conference on Space Optics — ICSO 2018, N. Karafolas, Z. Sodnik, and B. Cugny, Eds., 64, SPIE, Chania, Greece (2019).

[2] Cezard, N., Dolfi-Bouteyre, A., Durécu, A., Faure, B., Goular, D., Gustave, F., Hébert, P.-J., Lahyani, J., Le Gouët, J., Lemaître, F., Lombard, L., Patiño, W., Planchat, C. and Valla, M., "Recent advances on fiber-based laser and Lidar systems for future space-borne monitoring of greenhouse gas," International Conference on Space Optics — ICSO 2020, Z. Sodnik, B. Cugny, and N. Karafolas, Eds., 67, SPIE, Online Only, France (2021).

[3] Coddington, I., Newbury, N. and Swann, W., "Dual-comb spectroscopy," Optica **3**(4), 414 (2016).

[4] Cossel, K. C., Waxman, E. M., Giorgetta, F. R., Cermak, M., Coddington, I. R., Hesselius, D., Ruben, S., Swann, W. C., Truong, G.-W., Rieker, G. B. and Newbury, N. R., "Open-path dual-comb spectroscopy to an airborne retroreflector," Optica **4**(7), 724 (2017).

[5] Picqué, N. and Hänsch, T. W., "Frequency comb spectroscopy," Nature Photon **13**(3), 146–157 (2019).

[6] Parriaux, A., Hammani, K. and Millot, G., "Electro-optic frequency combs," Adv. Opt. Photon. **12**(1), 223 (2020).

[7] Deschênes, J.-D. and Genest, J., "Frequency-noise removal and on-line calibration for accurate frequency comb interference spectroscopy of acetylene," Appl. Opt. **53**(4), 731 (2014).

[8] Patiño, W. and Cézard, Nicolas., "Electro-optic frequency comb based IPDA lidar: assessment of speckle issues," Optics Express **30** (2022).

[9] Nicholson, J. W., DeSantolo, A., Yan, M. F., Wisk, P., Mangan, B., Puc, G., Yu, A. W. and Stephen, M. A., "High energy, 15723 nm pulses for CO_2 LIDAR from a polarization-maintaining, very-large-mode-area, Er-doped fiber amplifier," Opt. Express **24**(17), 19961 (2016).